Appl. Math. Mech. -Engl. Ed., **38**(7), 1019–1030 (2017)
DOI 10.1007/s10483-017-2220-6
©Shanghai University and Springer-Verlag
Berlin Heidelberg 2017

Applied Mathematics and Mechanics (English Edition)

Integration of a nonlinear energy sink and a piezoelectric energy harvester*

Xiang LI[1], Yewei ZHANG[1,2,†], Hu DING[1,3], Liqun CHEN[1,3,4]

1. Shanghai Institute of Applied Mathematics and Mechanics, Shanghai University, Shanghai 200072, China;
2. College of Aerospace Engineering, Shenyang Aerospace University, Shenyang 110136, China;
3. Shanghai Key Laboratory of Mechanics in Energy Engineering, Shanghai University, Shanghai 200072, China;
4. Department of Mechanics, Shanghai University, Shanghai 200444, China

Abstract A mechanical-piezoelectric system is explored to reduce vibration and to harvest energy. The system consists of a piezoelectric device and a nonlinear energy sink (NES), which is a nonlinear oscillator without linear stiffness. The NES-piezoelectric system is attached to a 2-degree-of-freedom primary system subjected to a shock load. This mechanical-piezoelectric system is investigated based on the concepts of the percentages of energy transition and energy transition measure. The strong target energy transfer occurs for some certain transient excitation amplitude and NES nonlinear stiffness. The plots of wavelet transforms are used to indicate that the nonlinear beats initiate energy transitions between the NES-piezoelectric system and the primary system in the transient vibration, and a 1:1 transient resonance capture occurs between two subsystems. The investigation demonstrates that the integrated NES-piezoelectric mechanism can reduce vibration and harvest some vibration energy.

Key words nonlinear energy sink (NES), nonlinear beat phenomenon, piezoelectric energy harvester, energy transition, NES-piezoelectric system

Chinese Library Classification V215.3$^+$4, O322
2010 Mathematics Subject Classification 34C15

1 Introduction

The study of vibration confinement by use of the nonlinear energy sink (NES) and energy harvesting through piezoelectric material has made great progress in the past several years.

The NES coupled to a dynamic system is composed of a small mass, damper, and cubic nonlinear stiffness spring without linear stiffness. Jiang et al.[1] utilized a piece of piano wire in the experiment to realize the pure cubic stiffness nonlinearity without a linear part. It has been proved that vibrational energy can be "pumped" to an NES[2–6]. The NES includes grounded and ungrounded configurations. It is able to perform over broadband frequency ranges, and

* Received Dec. 9, 2016 / Revised Mar. 14, 2017
Project supported by the National Natural Science Foundation of China (Nos. 11572182, 11232009, and 11402151) and the Natural Science Foundation of Liaoning Province (No. 2015020106)
† Corresponding author, E-mail: zhangyewei1218@126.com

transfer and dissipate significant input vibration energy[3–9]. Gendelman et al.[3] and Vakakis and Gendelman[4] investigated a 2-degree-of-freedom system including the NES, and stated that resonance capture contributed to energy pumping. Gendelman et al.[3] and McFarland et al.[10] proposed that the NES would work when the shock energy was more than a certain value. Lee et al.[11] studied the undamped and weakly damped system composed of a linear and nonlinear oscillator, analyzed the frequency-energy plot of the periodic orbits in the undamped system, and revealed that the NES could realize certain internal resonance with the linear part due to tuning itself during certain frequency-energy ranges. Kerschen et al.[12] focused on the study of the energy transfer mechanisms in a linear oscillator with the NES, and presented three types of energy transfer mechanisms including fundamental or subharmonic target energy transfer and target energy transfer initiated by nonlinear beats. They also pointed out that the damper was responsible for the irreversible energy transitions from the linear part to the NES. Kerschen et al.[11] and Georgiades et al.[12] both used wavelet transforms to analyze the harmonic components in the time history. Georgiades et al.[13] focused on the efficiency energy transfer of the NES, and used the energy transition measure to study the instantaneous energy transition between the NES and the structure. They adopted some signal processing methods such as wavelet transforms to analyze the strong or weak energy transfer. Ahmadabadi and Khadem[14] investigated the efficiency of grounded and ungrounded NES configurations, and showed that the ungrounded configuration dissipated the vibrational energy effectively. Gourdon et al.[15] researched theoretically, numerically, and experimentally the effective energy pumping for a system with a linear oscillator coupled with a nonlinear oscillator. Kremer and Liu[16] designed an energy harvesting system with the NES coupling the magnet.

It is beneficial to convert vibration energy to electricity, and vibration-based energy harvesting is an active research field[17–20]. Recently, nonlinearity is used to enhance energy harvesting[21–24]. Attempts to combine vibration reduction with energy harvesting for some structures have been made[25–27]. Chtiba et al.[25] designed an electromechanical model including a linear absorber and a piezoelectric device, and used this model to a simply support beam. Ahmadabadi and Khadem[26] designed optimally two electromechanical models composed of an NSE and a piezoelectric element for a beam. Zhang et al.[27] designed a kind of piezoelectric energy-harvesting device in the experiment, and demonstrated the possibility of realizing the dissipation and the harvesting of vibration energy. However, they did not focus on the energy transfer mechanism, which is still an open problem for integrating an NES and an energy harvester.

To explore the possible energy transfer mechanism in a combination of an NES and an energy harvester, the present investigation focuses on a 2-degree-freedom primary system with an NES-piezoelectric system. Some system parameters are chosen to achieve the absorbing and the harvesting of vibration energy simultaneously. Then, a numerical wavelet analysis is performed to determine the dominating frequency components in the response time history. The wavelet analysis reveals that the nonlinear beats can be regarded as the energy transfer mechanism between the primary system and the attached NES-piezoelectric system. The energy transition measure is calculated to examine the instantaneous energy transition between the primary system and the NES-piezoelectric system. The manuscript is organized as follows. Section 2 summarizes the methodology to propose a framework for the investigation. Section 3 presents the calculation investigations about the structure with the NES-piezoelectric system. Section 4 ends the manuscript with the concluding remarks.

2 Methodology

The energetics of a structure with an attachment is treated. The structure is a 2-degree-of-freedom linear system, and the attachment consists of an NES and a piezoelectric device. The NES and piezoelectric device are referred to as the NES-piezoelectric system, where the

structure is referred to as the primary system, and the primary system is subjected to a shock load.

The energy of the primary system will be partially dissipated by the dampers of the primary system and the NES, and partially harvested by the piezoelectric device. The Runge-Kutta algorithm is used to integrate the equations of motion. Based on the obtained solutions, the energy dissipation and harvesting are examined. The mass and nonlinear stiffness are designed to maximize the percentages of the input energy eventually dissipated by the NES damper, i.e.,

$$\eta_{\mathrm{NES}}(t) = \frac{W_{\mathrm{NES}}(t)}{W_{\mathrm{in}}} \times 100\%, \tag{1}$$

and harvested by the piezoelectric device, i.e.,

$$\eta_{\mathrm{piezo}}(t) = \frac{W_{\mathrm{piezo}}(t)}{W_{\mathrm{in}}} \times 100\%, \tag{2}$$

where $W_{\mathrm{NES}}(t)$ is the energy at the time t dissipated by the NES damper, $W_{\mathrm{piezo}}(t)$ is the energy at the time t harvested by the piezoelectric device, and W_{in} is the input transient excitation energy.

To ensure the energy balance, the percentage

$$\eta_{\mathrm{total}}(t) = \frac{W_{\mathrm{PS}}(t) + W_{\mathrm{NES}}(t) + W_{\mathrm{piezo}}(t)}{W_{\mathrm{in}}} \times 100\% \tag{3}$$

will be checked whether it tends to 1 or not when the time is large enough, where $W_{\mathrm{PS}}(t)$ is the energy at the time t dissipated by the primary system damping. The percentage of the energy transmitted into the NES-piezoelectric system without dissipation, i.e.,

$$\eta_{\text{NES-piezo}}(t) = \frac{T_{\mathrm{NES}}(t) + V_{\mathrm{NES}}(t) + V_{\mathrm{piezo}}(t)}{W_{\mathrm{in}}} \times 100\%, \tag{4}$$

where $T_{\mathrm{NES}}(t)$ and $V_{\mathrm{NES}}(t)$ are the kinetic energy and the elastic potential energy of the NES, respectively, and $V_{\mathrm{piezo}}(t)$ is the elastic potential energy of the piezoelectric device, should tend to 0. The percentage of the energy dissipated by the dampers of the primary system can be expressed as follows:

$$\eta_{\mathrm{PS}}(t) = \frac{W_{\mathrm{PS}}(t)}{W_{\mathrm{in}}} \times 100\%. \tag{5}$$

Numerical results are processed to analyze the energy transition between the NES-piezoelectric system and the primary system. The approach proposed by Lee et al.[11] and Kerschen et al.[12] for NES systems will be generalized to the NES-piezoelectric system. As an effective technique of the time-frequency analyses, wavelet transforms are used to analyze the data of transient responses. The plot of wavelet transforms is calculated to differentiate high and low wavelet transform amplitudes. The time histories of the main frequency components of the signals are analyzed according to the time-frequency figures with a particular focus on the energy transition in the frequency region.

The energy transition measure, a significant computational measure proposed by Georgiades et al.[13] for NES systems, is extended to analyze the instantaneous energy transition between the primary system and the NES-piezoelectric system. The energy flowing back or forth between the primary system and the NES-piezoelectric system, denoted as $E_{\mathrm{trans}}(t)$, can be expressed as follows:

$$E_{\mathrm{trans}}(t) = \Delta T_{\mathrm{NES}}(t) + \Delta V_{\mathrm{NES}}(t) + \Delta W_{\mathrm{NES}}(t) + \Delta V_{\mathrm{piezo}}(t) + \Delta W_{\mathrm{piezo}}(t), \tag{6}$$

where the operator Δ represents the difference between two adjacent time integration steps, $W_{\mathrm{NES}}(t)$ is the energy dissipated by the NES damper, $V_{\mathrm{piezo}}(t)$ is the elastic potential energy of the piezoelectric device, and $W_{\mathrm{piezo}}(t)$ is the energy harvested by the piezoelectric device. Obviously, positive $E_{\mathrm{trans}}(t)$ indicates that the transient energy is transferred from the primary system to the NES-piezoelectric system, and vice versa. Positive and negative spikes of $E_{\mathrm{trans}}(t)$ are presented to check the energy transitions.

3 Structure with the NES-piezoelectric system

As shown in Fig. 1, the piezoelectric device is embedded between the NES mass and the structure. The primary system is subjected to a shock load $F(t)$, which is expressed as Eq. (8). The pure cubic stiffness nonlinearity can be completely realized by employing a type of piano wire. The equations of motion are given as follows:

$$\begin{cases} m_1\ddot{x}_1 + c_1(\dot{x}_1 - \dot{x}_2) + k_1(x_1 - x_2) = F(t), \\ m_2\ddot{x}_2 + c_1(\dot{x}_2 - \dot{x}_1) + c_2\dot{x}_2 + c_3(\dot{x}_2 - \dot{x}_3) + k_1(x_2 - x_1) + k_2x_2 \\ \quad + k_3(x_2 - x_3)^3 + k_{\mathrm{p}}(x_2 - x_3) - \theta u = 0, \\ m_3\ddot{x}_3 + c_3(\dot{x}_3 - \dot{x}_2) + k_3(x_3 - x_2)^3 + k_{\mathrm{p}}(x_3 - x_2) + \theta u = 0, \\ -\theta(\dot{x}_3 - \dot{x}_2) + C_{\mathrm{p}}\dot{u} + \dfrac{1}{R}u = 0, \end{cases} \tag{7}$$

where m_1, m_2, and m_3 are the first rigid mass, the second rigid mass, and the NES mass, respectively. x_1, x_2, and x_3 are the displacements of the first rigid, the second rigid, and the NES relative to the ground, respectively. c_1, c_2, and c_3 are the linear damping coefficients of the first rigid, the second rigid, and the NES, respectively. k_1 and k_2 are the linear spring stiffness coefficients, while k_3 is the cubic nonlinear stiffness coefficient. k_{p} and C_{p} are the equivalent linear stiffness and the equivalent capacitance of the piezoelectric device, respectively, R is the external resistance, u is the output voltage, and θ is the electromechanical coupling coefficient. The primary system is subjected to a shock load $F(t)$ defined by

$$F(t) = \begin{cases} A\sin\left(\dfrac{2\pi}{T}t\right), & 0 \leqslant t \leqslant \dfrac{T}{2}, \\ 0, & t > \dfrac{T}{2}, \end{cases} \tag{8}$$

where $T = 0.1T_1$ in which T_1 is the corresponding period of the first mode of the primary system, and A is the transient excitation amplitude.

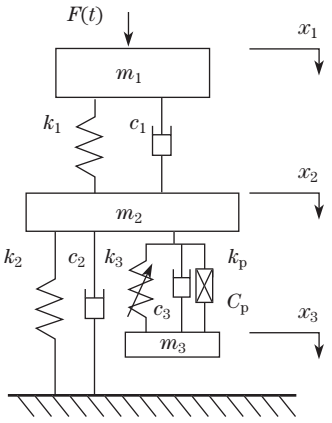

Fig. 1 2-degree-of-freedom primary system with the NES-piezoelectric system

In the following research work, the time discretization of the nonlinear ordinary differential equations is carried out in the time history. It is based on the 4th-order Runge-Kutta algorithm with the fixed time interval $\tau = 1\times10^{-4}$ s. The parameters of the 2-degree-of-freedom primary system are

$$\begin{cases} m_1 = 60\,\mathrm{kg}, \quad m_2 = 12\,\mathrm{kg}, \quad k_1 = 1.867\,7\times10^6\,\mathrm{N\cdot m^{-1}}, \\ k_2 = 2.134\,6\times10^6\,\mathrm{N\cdot m^{-1}}, \quad c_1 = 3\times10^2\,\mathrm{N\cdot s\cdot m^{-1}}, \quad c_2 = 10\,\mathrm{N\cdot s\cdot m^{-1}}. \end{cases}$$

These data are based on the work of Yang et al.[28]. The parameters of the piezoelectric device are

$$k_\mathrm{p} = 1\times10^3\,\mathrm{N\cdot m^{-1}}, \quad R = 8.2\times10^5\,\Omega, \quad C_\mathrm{p} = 1\times10^{-8}\,\mathrm{F}, \quad \theta = 1\times10^{-3}\,\mathrm{C\cdot m^{-1}}.$$

The effects of the NES parameters on absorbing the input energy passively will be investigated in order to improve the design of the NES. The energy dissipated by the NES damper is

$$W_\mathrm{NES}(t) = \int_0^t c_3(\dot{x}_3(\tau) - \dot{x}_2(\tau))^2\mathrm{d}\tau. \tag{9}$$

The energy harvested by the piezoelectric device is

$$W_\mathrm{piezo}(t) = \int_0^t \frac{u^2(\tau)}{R}\mathrm{d}\tau. \tag{10}$$

The energy input by the shock force is

$$W_\mathrm{in} = \int_0^{\frac{T}{2}} F(\tau)\dot{x}_1(\tau)\mathrm{d}\tau. \tag{11}$$

Substituting Eqs. (9), (10), and (11) into Eqs. (1) and (2) yields the percentages of the total input energy eventually dissipated by the NES damper (η_NES) and harvested by the piezoelectric device (η_piezo), respectively. In these equations, t is chosen as t_final, which is the interval of the time from the vibration beginning to its end. The damper of the NES is chosen as $c_3 = 5\,\mathrm{N\cdot s\cdot m^{-1}}$. The contour plots of η_NES and η_piezo as functions of the transient excitation amplitude A and the NES nonlinear stiffness k_3 are, respectively, shown in Figs. 2(a) and 2(b). In Fig. 2, different values of the shock amplitude and the NES nonlinear stiffness are considered, i.e., $A \in[1\times10^3,\ 5\times10^4]$ and $k_3 \in[1\times10^8,\ 1\times10^9]$. For a certain damper of the NES, the red regions in Fig. 2 mean that obvious target energy transfer occurs including the transformation into the electric energy. In particular, for these regions, the percentage of the harvested energy is also increased since the piezoelectric device is connected to the NES. Besides, the nonlinear stiffness has a significant effect on strong target energy transfer when the input energy is more than some certain value. Similarly, in Fig. 3, different values of the shock amplitude and the NES mass are considered, i.e., $A \in[1\times10^3,\ 5\times10^4]$ and $m_3 \in[3.6, 6]$, where the values of the NES mass should satisfy the requirement that the nonlinear absorber mass is more than 1/20 and less than 1/10 of the primary system mass. It is also revealed in Figs. 2 and 3 that the relatively strong dissipated energy and harvested energy can occur only when the shock energy is more than a certain value. The requirement of large enough shocks for the work of the NES has been observed in Refs. [3] and [10] without piezoelectric devices.

It is worth of discussing the relationship between the nonlinear cubic stiffness of the NES and the voltage of the piezoelectric device with other fixed structure parameters. According to the 4th-order Runge-Kutta algorithm, the voltage response curve in the time history is depicted in Fig. 4 with the NES parameters $k_3 = 3.85\times10^8\,\mathrm{N\cdot m^{-3}}$, $c_3 = 5\,\mathrm{N\cdot s\cdot m^{-1}}$, and $m_3 = 3.8\,\mathrm{kg}$. In Fig. 4, the black solid line represents the voltage response of the piezoelectric device

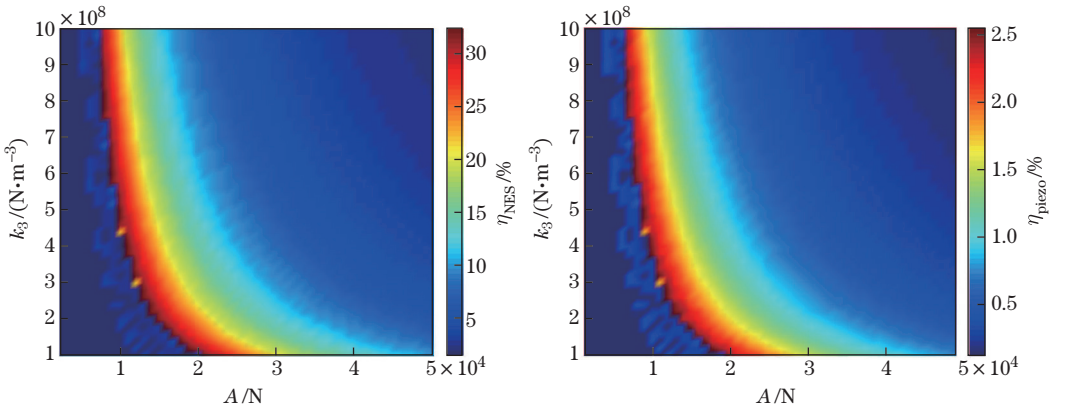

(a) Percentage about dissipated energy (b) Percentage about harvested energy

Fig. 2 Contour plots of the coefficient percentage of transient excitation energy eventually dissipated by the NES damper and harvested by the piezoelectric device as a function of the transient excitation amplitude and the NES nonlinear stiffness

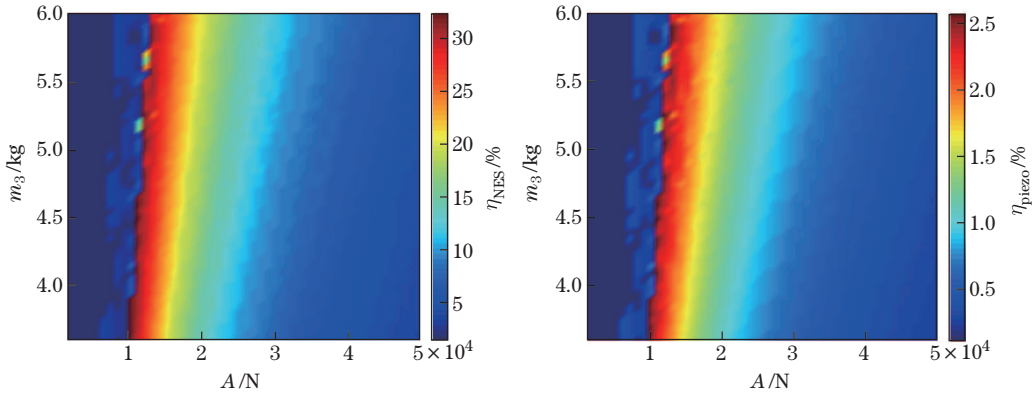

(a) Percentage about dissipated energy (b) Percentage about harvested energy

Fig. 3 Contour plots of the mass percentage of transient excitation energy eventually dissipated by the NES damper and harvested by the piezoelectric device as a function of the transient excitation amplitude and the NES mass

in the time history, while the two red dashed dotted lines remark the envelope of the corresponding voltage response curve. Obviously, the voltage response curve in the time history is detailed and complicated, and it is not visual and convenient to express the relationship between the nonlinear cubic stiffness and the output voltage of the piezoelectric device. The envelope of the voltage response curve in Fig. 4 expresses the voltage amplitude magnitude and tendency visually and briefly to some extent. Therefore, the envelopes of the corresponding voltage response curves under different nonlinear cubic stiffness parameters of the NES are performed to investigate the relationship between the nonlinear stiffness and the voltage of the piezoelectric device.

Figure 5 shows the envelopes of the corresponding voltage response curves under different cubic stiffness parameters. Specifically, the parameters of the nonlinear cubic stiffness k_3 are $2\times10^8\,\mathrm{N\cdot m^{-3}}$, $3.85\times10^8\,\mathrm{N\cdot m^{-3}}$, and $9\times10^8\,\mathrm{N\cdot m^{-3}}$. Their envelopes of the voltage response curves are represented by black short dotted lines, red solid lines, and blue dashed dotted lines, respectively. Compared with the parameter $k_3 = 3.85\times10^8\,\mathrm{N\cdot m^{-3}}$, the voltage amplitudes

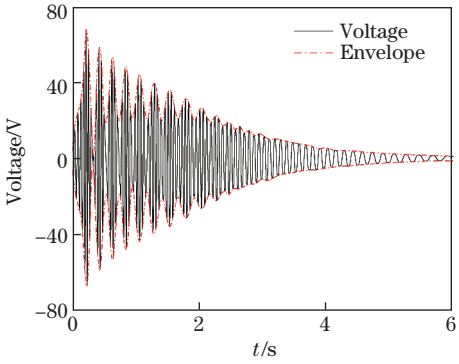

Fig. 4 Voltage response curve and the corresponding envelope in the time history with the NES parameters $k_3 = 3.85\times10^8\,\mathrm{N\cdot m^{-3}}$, $c_3 = 5\,\mathrm{N\cdot s\cdot m^{-1}}$, and $m_3 = 3.8\,\mathrm{kg}$

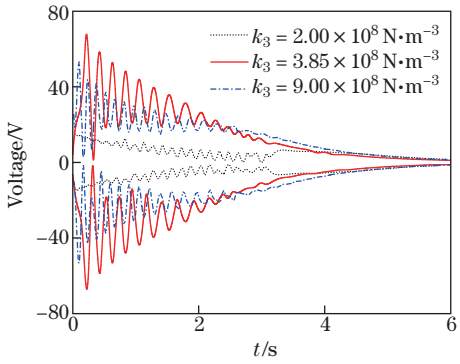

Fig. 5 Envelopes of the voltage response curves in the time history with different parameters of the nonlinear cubic stiffness

of the piezoelectric device decrease with the increase in the nonlinear stiffness. The similar tendency, that the voltage amplitudes will decrease, can be obtained when the values of the nonlinear stiffness become small. It is indicated that a larger output voltage of the piezoelectric device can be acquired through adjusting the value of the nonlinear cubic stiffness of the NES.

Then, investigate the distribution of the input shock energy when the strong target energy transfer occurs. The NES damper is chosen to be $c_3 = 5\,\mathrm{N\cdot s\cdot m^{-1}}$. Other two parameters of the NES are $m_3 = 3.8\,\mathrm{kg}$ and $k_3 = 3.85\times10^8\,\mathrm{N\cdot m^{-3}}$. The transient excitation amplitude is chosen to be $A = 1\times10^4\,\mathrm{N}$. Since the kinetic energy and the elastic potential energy of the NES are

$$T_{\mathrm{NES}}(t) = \frac{1}{2}m_3\dot{x}_3^2(t), \tag{12}$$

$$V_{\mathrm{NES}}(t) = \frac{1}{4}k_3(x_3(t) - x_2(t))^4, \tag{13}$$

the elastic potential energy of the piezoelectric device is

$$V_{\mathrm{piezo}}(t) = \frac{1}{2}k_{\mathrm{p}}(x_3(t) - x_2(t))^2. \tag{14}$$

Substituting Eqs. (11)–(14) into Eq. (4) yields the percentage of the energy transmitted into the NES-piezoelectric system without dissipation. The percentage of the instantaneous input energy transmitted into the NES-piezoelectric system is shown in Fig. 6(b) with the enlargement of the initial time interval in Fig. 6(a). This percentage tends eventually to zero. Figures 7(a) and 7(b) depict the percentages of the captured energy dissipated by the NES damper $\eta_{\mathrm{NES}}(t)$ and harvested by the piezoelectric device $\eta_{\mathrm{piezo}}(t)$, respectively. Even if the transient input energy is stored in the 2-degree-of-freedom primary system at the initial moment, a part of the input energy quickly flows between the NES-piezoelectric system and the primary system. In Figs. 7(a) and 7(b), in the beginning, about 38% transient shock energy exists in the NES-piezoelectric system, and thereafter this percentage reduces to approximate 0.80%. These imply that a nonlinear beat phenomenon takes place in this NES-piezoelectric system. Because of this phenomenon, the energy transition between two subsystems is reversible[11–12]. A similar situation occurs in the system with an energy harvester. Under this energy transfer mechanism, the captured shock energy is dissipated by the NES damper and especially harvested by the piezoelectric device, which amount to about 32.39% and 2.54%, respectively. It is illustrated that, a part of shock energy can be transferred to the NES-piezoelectric system and this energy

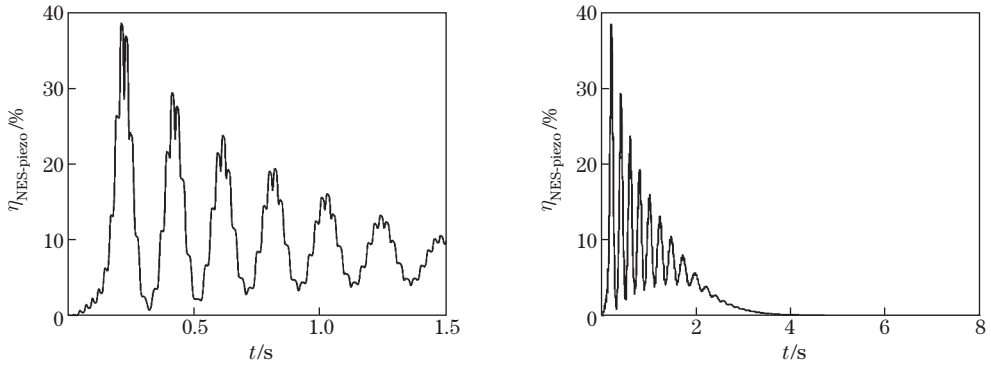

(a) 0 s –1.5 s (b) 0 s –8 s

Fig. 6 Percentage of instantaneous energy in the NES-piezoelectric system

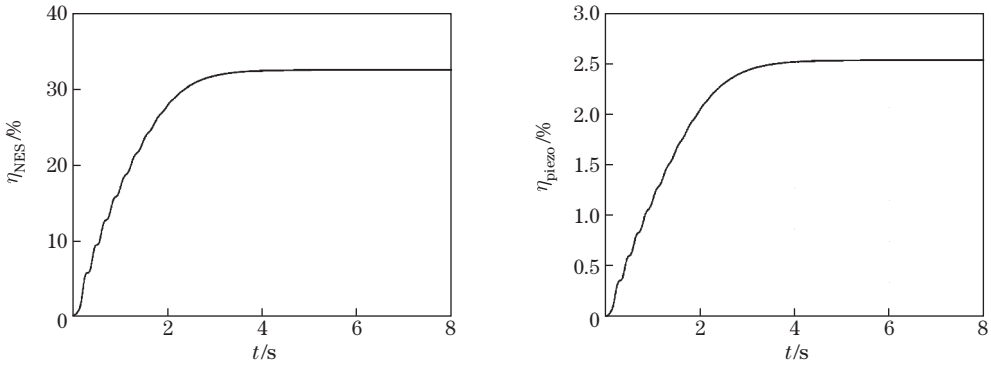

(a) Percentage of dissipated energy (b) Percentage of harvested energy

Fig. 7 Percentage of energy dissipated or harvested by the NES-piezoelectric system

is eventually dissipated by the NES damper and particularly harvested or stored as electric energy by the piezoelectric device.

The energy dissipated by the dampers of the primary system is expressed as follows:

$$W_{\text{PS}}(t) = \int_0^{t_{\text{final}}} c_1(\dot{x}_1(\tau) - \dot{x}_2(\tau))^2 \mathrm{d}\tau + \int_0^{t_{\text{final}}} c_2 \dot{x}_2^2(\tau) \mathrm{d}\tau. \tag{15}$$

The percentage of the total input energy eventually dissipated by the dampers of the primary system can be obtained by substituting Eqs. (11) and (15) into Eq. (5). The percentage of the dissipated energy by the dampers of the primary system $\eta_{\text{PS}}(t)$ is depicted in Fig. 8. The percentage of the input energy eventually dissipated by the dampers of the primary system is about 65.21%. According to Eq. (3), the calculated value of η_{total} is about 1.001 4. The calculation error of the whole numerical method is about 1.4‰. It means that the calculation error is very small, and the calculation methods and process are reasonable.

Furthermore, wavelet transforms are used to analyze the transient energy transitions initiated by the nonlinear beats. The Morlet mother wavelet is utilized to process the corresponding signal. As we know, the first-order natural frequency of the primary system is about 20.05 Hz. Figure 9 depicts the transient displacement responses of the mass 1 in the primary system and its wavelet transform spectra.

Figure 10 describes the transient relative displacement responses among the primary system, the NES-piezoelectric system, and the corresponding wavelet transform spectra. As depicted

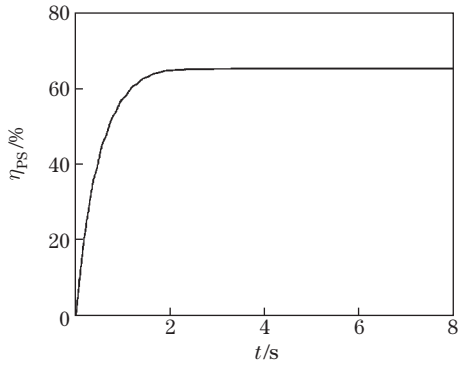

Fig. 8 Percentage of dissipated energy by the dampers of the primary system

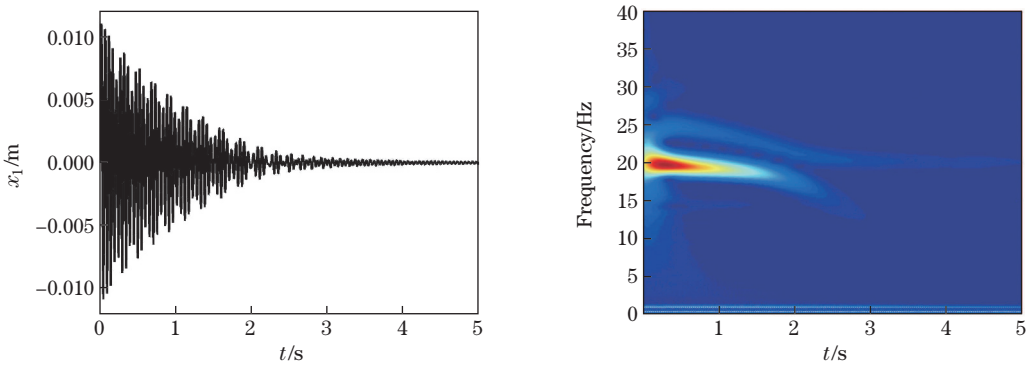

(a) Transient displacement responses (b) Wavelet transforms

Fig. 9 Responses of the mass 1 in the primary system

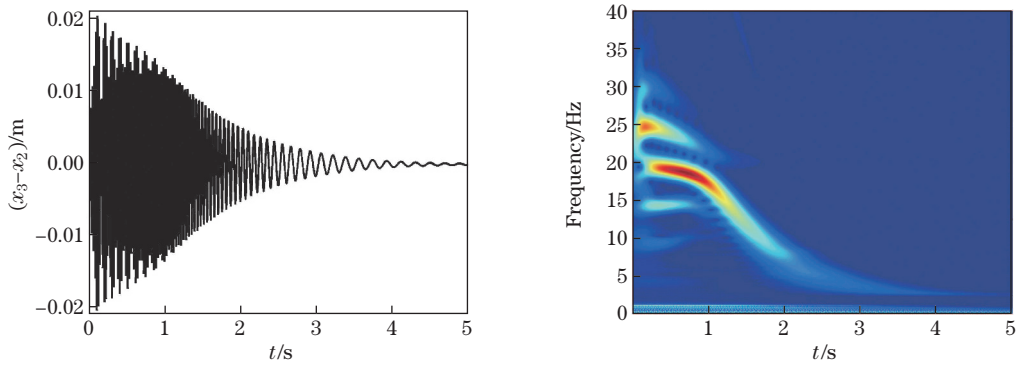

(a) Transient relative responses (b) Wavelet transforms

Fig. 10 Relative responses between the primary system and the NES-piezoelectric system

in Fig. 9(b), the main frequency component of the 2-degree-of-freedom primary system is approximately 20 Hz, while the transient response of the NES-piezoelectric system has two main frequency components, i.e., about 25 Hz and 20 Hz, which is shown in Fig. 10(b). After about 1 s, the transient response of the NES-piezoelectric system has one main frequency component, i.e., about 20 Hz. Following this, the dynamics shows a 1:1 transient resonance capture between

the NES-piezoelectric system and the primary system. Since the input energy further decreases due to the damping dissipation and harvesting energy, the escaping phenomenon from resonance capture occurs. The frequency component of the NES-piezoelectric system response eventually manifests in the low frequency range. As mentioned above this section, this is because of the existence of the linear equivalent stiffness in the NES-piezoelectric system.

The energy transition measure is adopted to study the instantaneous energy transition between the 2-degree-freedom primary system and the NES-piezoelectric system. Substituting Eqs. (9), (10), (12), (13), and (14) into Eq. (12) yields the transition energy between the two subsystems $E_{\text{trans}}(t)$. The NES parameters, i.e., $m_3 = 3.8\,\text{kg}$, $k_3 = 3.85\times10^8\,\text{N}\cdot\text{m}^{-3}$, and $c_3 = 5\,\text{N}\cdot\text{s}\cdot\text{m}^{-1}$, are chosen to study the input energy transfer histories. Figure 11 shows the energy transition histories between the 2-degree-freedom primary system and the NES-piezoelectric system. Figures 11(a)–11(d) present the total energy transitions, the mechanical energy transitions, the kinetic and potential energy transitions, and the dissipated and harvested energy transitions, respectively. There are similar conclusions from these figures. In Fig. 11(a), the positive values mean the energy transition from the primary system to the NES-piezoelectric system, and vice versa. Due to the nonlinear beat phenomena, positive and negative spikes both exist in the initial time of motion, and continue to exit with time going on because of the relatively weak capability of dissipating energy (32.40%) or the harvesting energy (2.54%). As depicted in Figs. 11(c) and 11(d), the instantaneous transition of the mechanical energy in the NES-piezoelectric system is the main part compared with that of the dissipated and harvested energy.

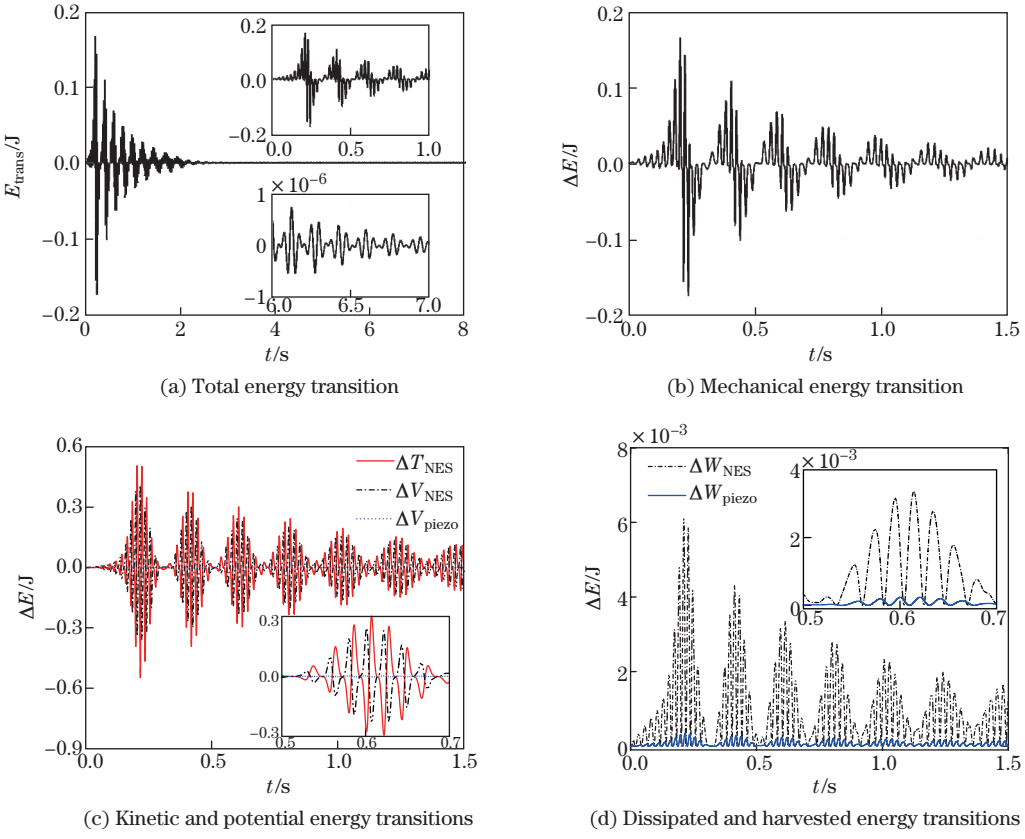

(a) Total energy transition

(b) Mechanical energy transition

(c) Kinetic and potential energy transitions

(d) Dissipated and harvested energy transitions

Fig. 11 Energy transitions between the primary system and the NES-piezoelectric system

4 Conclusions

This work demonstrates the mechanisms of absorbing or dissipating and harvesting the nonlinear energy simultaneously in a system with the NES and piezoelectric device. The numerical evidences based on the 4th-order Runge-Kutta algorithm are presented in the investigation. With some certain ranges of the transient excitation amplitude and the NES nonlinear stiffness, the relatively strong target energy, including dissipated energy and harvested energy, transfer occurs. The modelling and simulations reveal the possibility of reducing vibration as well as harvesting vibration energy via the integration of an NES and a piezoelectric device. Experiments should be conducted to examine this theoretical possibility.

Wavelet transforms are used to illustrate that a nonlinear beat phenomenon initiates the energy transitions between the NES-piezoelectric system and the primary system in the transient vibration. A 1:1 transient resonance capture occurs between two subsystems. As the input energy further decreases due to the damping dissipation and harvesting energy, the phenomenon of escaping from resonance capture occurs. The capture energy is eventually dissipated by the NES damper, and especially harvested by the piezoelectric device. The energy transition measure is numerically determined to examine the instantaneous energy transition between the 2-degree-freedom primary system and the NES-piezoelectric system. The positive and negative spikes of E_{trans} are presented, and continuous energy transitions will occur when the target energy transfer is initiated by nonlinear beats.

References

[1] Jiang, X., McFarland, D. M., Bergman, L. A., and Vakakis, A. F. Steady state passive nonlinear energy pumping in coupled oscillators: theoretical and experimental results. *Nonlinear Dynamics*, **33**(1), 87–102 (2003)

[2] Vakakis, A. F. Shock isolation through the use of nonlinear energy sinks. *Journal of Vibration and Control*, **9**(1-2), 79–93 (2003)

[3] Gendelman, O., Manevitch, L. I., Vakakis, A. F., and M'Closkey, R. Energy pumping in nonlinear mechanical oscillators: part I, dynamics of the underlying Hamiltonian systems. *Journal of Applied Mechanics*, **68**(1), 34–41 (2001)

[4] Vakakis, A. F. and Gendelman, O. Energy pumping in coupled mechanical oscillators: part II, resonance capture. *Journal of Applied Mechanics*, **68**(1), 42–48 (2001)

[5] Vakakis, A. F. Inducing passive nonlinear energy sinks in linear vibrating systems. *Journal of Vibration and Acoustics*, **123**(3), 324–332 (2001)

[6] Lee, Y. S., Vakakis, A. F., Bergman, L. A., McFarland, D. M., Kerschen, G., Nucera F., Tsakirtzis, S., and Panagopoulos, P. N. Passive non-linear targeted energy transfer and its applications to vibration absorption: a review. *Proceedings of the Institution of Mechanical Engineers*, **222**(2), 77–134 (2008)

[7] Gourdon, E. and Lamarque, C. H. Nonlinear energy sink with uncertain parameters. *Journal of Computational and Nonlinear Dynamics*, **1**(3), 187–195 (2006)

[8] Al-Shudeifat, M. A. Highly efficient nonlinear energy sink. *Nonlinear Dynamics*, **76**(4), 1905–1920 (2014)

[9] Lamarque, C. H., Thouverez, F., Rozier, B., and Dimitrijevic, Z. Targeted energy transfer in a 2-DOF mechanical system coupled to a non-linear energy sink with varying stiffness. *Journal of Vibration and Control* (2015) DOI 10.1177/1077546315618540

[10] McFarland, D. M., Bergman, L. A., and Vakakis, A. F. Experimental study of non-linear energy pumping occurring at a single fast frequency. *International Journal of Non-Linear Mechanics*, **40**(6), 891–899 (2005)

[11] Lee, Y. S., Kerschen, G., Vakakis, A. F., Panagopoulos, P., Bergman, L., and McFarland, D. M. Complicated dynamics of a linear oscillator with a light, essentially nonlinear attachment. *Physica D: Nonlinear Phenomena*, **204**(1), 41–69 (2005)

[12] Kerschen, G., Lee, Y. S., Vakakis, A. F., McFarland, D. M., and Bergman, L. A. Irreversible passive energy transfer in coupled oscillators with essential nonlinearity. *Journal on Applied Mathematics*, **66**(2), 648–679 (2006)

[13] Georgiades, F., Vakakis, A. F., and Kerschen, G. Broadband passive targeted energy pumping from a linear dispersive rod to a lightweight essentially non-linear end attachment. *International Journal of Non-Linear Mechanics*, **42**(5), 773–788 (2007)

[14] Ahmadabadi, Z. N. and Khadem, S. E. Nonlinear vibration control of a cantilever beam by a nonlinear energy sink. *Mechanism and Machine Theory*, **50**, 134–149 (2012)

[15] Gourdon, E., Lamarque, C. H., and Pernot, S. Contribution to efficiency of irreversible passive energy pumping with a strong nonlinear attachment. *Nonlinear Dynamics*, **50**(4), 793–808 (2007)

[16] Kremer, D. and Liu, K. A nonlinear energy sink with an energy harvester: transient responses. *Journal of Sound and Vibration*, **333**(20), 4859–4880 (2014)

[17] Sodano, H. A. and Inman, D. J. A review of power harvesting from vibration using piezoelectric materials. *The Shock and Vibration Digest*, **36**(3), 197–206 (2004)

[18] Anton, S. R. and Sodano, H. A. A review of power harvesting using piezoelectric materials (2003–2006). *Smart Materials and Structures*, **16**(3), R1–R21 (2007)

[19] Zhu, D., Tudor, M. J., and Beeby, S. P. Strategies for increasing the operating frequency range of vibration energy harvesters: a review. *Measurement Science and Technology*, **21**(2), 022001 (2009)

[20] Tang, L. H., Yang, Y. W., and Soh, C. K. Toward broadband vibration-based energy harvesting. *Journal of Intelligent Material Systems and Structures*, **21**(18), 1867–1897 (2010)

[21] Daqaq, M. F., Masana, R., Erturk, A., and Quinn, D. D. On the role of nonlinearities in vibratory energy harvesting: a critical review and discussion. *Applied Mechanics Reviews*, **66**(4), 040801 (2014)

[22] Harne, R. L. and Wang, K. W. A review of the recent research on vibration energy harvesting via bistable systems. *Smart Materials and Structures*, **22**(2), 023001 (2013)

[23] Pellegrini, S. P., Tolou, N., Schenk, M., and Herder, J. L. Bistable vibration energy harvesters: a review. *Journal of Intelligent Material Systems and Structures*, **24**, 1303–1312 (2012)

[24] Chen, L. Q. and Jiang, W. A. Internal resonance energy harvesting. *Journal of Applied Mechanics*, **82**(3), 031004 (2015)

[25] Chtiba, M. O., Choura, S., and El-Borgi, S. Vibration confinement and energy harvesting in flexible structures. *Journal of Sound and Vibration*, **329**(3), 261–276 (2010)

[26] Ahmadabadi, Z. N. and Khadem, S. E. Nonlinear vibration control and energy harvesting of a beam using a nonlinear energy sink and a piezoelectric device. *Journal of Sound and Vibration*, **333**(19), 4444–4457 (2014)

[27] Zhang, Y., Tang, L. H., and Liu, K. F. Piezoelectric energy harvesting with a nonlinear energy sink. *Proceedings of SPIE*, **9431**, 94310R (2015)

[28] Yang, K., Zhang, Y. W., Ding, H., Yang, T. Z., Li, Y., and Chen, L. Q. Nonlinear energy sink for whole-spacecraft vibration reduction. *Journal of Vibration and Acoustics of the ASME*, **139**(2), 021011 (2017)